Chemical degradation, yields, and interactions of lignocellulosic compounds of poplar wood during dilute acid pretreatment assessed from a comprehensive data set

Julien du Pasquier, Gabriel Paës, Patrick Perré

Industrial Crops & Products 215 (2024) 118643

Contents lists available at ScienceDirect

Industrial Crops & Products

journal homepage: www.elsevier.com/locate/indcrop

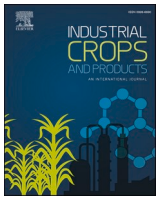

Chemical degradation, yields, and interactions of lignocellulosic compounds of poplar wood during dilute acid pretreatment assessed from a comprehensive data set

Julien du Pasquier [a,b], Gabriel Paës [a,*], Patrick Perré [b]

[a] Université de Reims Champagne-Ardenne, INRAE, FARE, UMR A 614, Reims 51100, France
[b] Université Paris-Saclay, CentraleSupélec, Laboratoire de Génie des Procédés et Matériaux, Centre Européen de Biotechnologie et de Bioéconomie (CEBB), Pomacle 51110, France

ARTICLE INFO

Original content: Chemical composition of solid and liquid phases resulting from dilute acid pretreatment of poplar wood under different conditions (Original data)

Keywords:
Lignocellulosic biomass
Biorefinery
Optimization
Regression
Chemical reaction

ABSTRACT

To optimize and guide future valorization of lignocellulosic biomass (LB) in biorefinery into different platform molecules, this work analyses a broad data set to provide a comprehensive overview of the chemical evolution sequences and interactions between different biomass compounds during pretreatment. For this purpose, a comprehensive dataset with a wide range of dilute acid pretreatment (DAP) conditions (2–60 min, 120–190°C, 0–4%wt H_2SO_4) and severity (Combined Severity Factor (CSF) 0–4) was used. This dataset gathers the chemical composition of 38 DAP-treated samples for 12 compounds (sugars, inhibitors, and lignin) in the solid residue and the liquid phase. All these data were related to the CSF value, so that kinetics are proposed to describe the evolution and quantify the degradation pathways of the C5 and C6-related compounds. All mathematical equations derived from this analysis are provided to the scientific community as supplementary material. The resulting comprehensive reaction scheme can thus be considered as a relevant guide to define the most appropriate DAP conditions depending on the expected objective of the pretreatment. In the case of enzymatic hydrolysis to release monosaccharides, CSFs from 2.0 to 2.5 reveal to be the most appropriate pretreatment conditions, while to produce furfural, a CSF slightly lower than 3 is more adapted. CSFs above 3 should be avoided since they lead to massive losses of polysaccharides.

1. Introduction

To face global warming, the emerging bioeconomy seeks to develop sustainable energy sources. Among them, this work focuses on the use of lignocellulosic biomass (LB) as a renewable carbon source, via the fermentation of its major constituent, cellulose, into biofuels such as bioethanol and other biochemicals (Yoo et al., 2020). Despite accounting for only 0.6% of the global energy mix for a total of 124 billion liters of bioethanol produced in 2021, LB could be much more developed with an estimate of 442 billion liters and 2.1% of the global energy mix (Chen et al., 2021; RFA, 2023; Ritchie et al., 2022). This development would also make it possible to move from edible resources based on starch and sugar which compete with the food industry, to LB-based resources based on industrial and forest wastes and co-products (Chen et al., 2021).

Indeed, cellulose, a polysaccharide composed of glucose units (linear β-1,4-glucan chains) (Chundawat et al., 2011), is present in the wall of support tissues of plants. Its crystalline structure forms micro-fibrils and fibrils, which are themselves embedded in a matrix composed of hemicelluloses, a mixture of branched pentose and hexose units, and lignin, a complex polyphenol heteropolymers (Becker and Wittmann, 2019; Chundawat et al., 2011; Pu et al., 2013). These two molecules, which are also of interest in the fields of chemicals, materials, fuels, and healthcare products (Acosta et al., 2021; Becker and Wittmann, 2019), physically prevent the enzymes from accessing the cellulose, and must therefore be degraded or removed to improve its accessibility. All these properties are part of a phenomenon called recalcitrance (Chundawat et al., 2011; Pu et al., 2013), which brings together all the physical and chemical properties of LB preventing the access and action of the enzyme on the cellulose (Beig et al., 2021). This makes its depolymerization into

Abbreviations: LB, Lignocellulosic biomass; DAP, Dilute acid pretreatment; HMF, Hydroxymethylfurfural; DMi, Initial dry matter; DMf, Final dry matter.

* Corresponding author.
E-mail address: gabriel.paes@inrae.fr (G. Paës).

https://doi.org/10.1016/j.indcrop.2024.118643
Received 20 February 2024; Received in revised form 9 April 2024; Accepted 27 April 2024
Available online 8 May 2024

glucose monomers by enzymatic hydrolysis very complicated.

To increase the efficiency of hydrolysis, a pretreatment of the LB is necessary (Tan et al., 2021). There are several types of pretreatments (physical, physico-chemical, chemical, and biological (Beig et al., 2021) but this article will focus mainly on a physico-chemical, dilute acid pretreatment (DAP). It consists in bringing the LB into contact with an acidic liquid medium (<10% wt), at high temperatures (120–210°C) and for variable times (from a few minutes to several hours) in a reactor under pressure (Beig et al., 2021; du Pasquier et al., 2023a). This pretreatment has already shown its potential in terms of chemical and economic efficiency, but it must be also improved to reduce the production of inhibitors limiting the action of enzymes, as well as its cost (du Pasquier et al., 2023a). But most of the articles published on DAP present reduced fields of study, changing only one or two factors at a time and analyzing only a few compounds (du Pasquier et al., 2023a). This prevents the emergence of a global interpretation of the effect of DAP and is a real obstacle to significant advances in quantifying the mechanisms involved in LB degradation by DAP.

The purpose of this article is therefore to increase the knowledge of the DAP thanks to the exploitation of a unique dataset representing an unprecedented large range of tested conditions (2–60 min, 120–190°C, 0–6.8%wt H_2SO_4). This dataset, generated in a previous article and fully accessible (du Pasquier, 2022; du Pasquier et al., 2023b), has been used to study the effect of the combined severity factor (CSF) on the kinetics of several poplar (*Populus tremula x Populus alba* hybrid) wood compounds. Regressions have been carried out on all the data and made it possible to visualize the kinetics of production and degradation of 12 different chemical species. Thanks to the aggregation of all these data, this article provides a comprehensive overview of the evolution of the chemical kinetics and mass balance of poplar wood compounds exposed to DAP, which to our knowledge is unprecedented in terms of the range of severities covered and the number of chemical species measured. These results will help in the choice of DAP conditions and the severity to be applied to the LB for various processes, whether to directly produce a specific platform molecules or to reduce the recalcitrance of the biomass prior to enzymatic hydrolysis for glucose production.

2. Materials and methods

2.1. Dataset generation

The data used in this work come from a dataset established in an earlier work and accessible online (du Pasquier, 2022). The sampling, sample processing and chemical analysis of the samples that made it possible to obtain these data were precisely described in a corresponding publication and will not be presented here (du Pasquier et al., 2023b).

2.2. Chemical analysis

The methods used to carry out the chemical analyzes have been described in a previous publication (du Pasquier et al., 2023b; Kim et al., 2021). This made it possible to obtain data on the evolution of solid poplar residues (solid fraction) and on the evolution of compounds solubilized in the acid solution used for pretreatment (liquid fraction). The solid fraction was analyzed for its composition in hemicelluloses, cellulose, and lignin, while the liquid fraction was analyzed for the amount of xylose, glucose, furfural, HMF, acetic acid, formic acid, levulinic acid and succinic acid. All compound contents are expressed as a percentage per 100 g of initial dry matter before pretreatment (%DMi).

2.3. Spectral analysis

The initial chemical data was completed by spectral analyses, also available in the du Pasquier (2022). The samples, reduced to powder after acid neutralization and washing, were analyzed by colorimetry and spectrofluorescence.

2.3.1. Colorimetry

For colorimetry, 3 measurements were carried out for each pretreated sample and for 5 raw samples (Chromometer CR-400, Konica Minolta, Japan). The 3 values obtained (L*, a* and b*) were averaged for each sample, and an average of the 5 raw samples was also made. Color distance ΔE from raw poplar wood was calculated by following Eq. 1, where ΔL*, Δa* and Δb* are the differences obtained by subtraction between raw and pretreated samples.

$$\Delta E = \sqrt{\Delta L^{*^2} + \Delta a^{*^2} + \Delta b^{*^2}} \quad (1)$$

2.3.2. Spectrofluorescence

For spectrofluorescence, the samples were excited between 250 and 450 nm, and the emitted autofluorescence was measured between 350 and 550 nm (Spectrofluorometer FP-8300, Jasco, France). Over the entire spectral area studied, the maximum intensity of emitted autofluorescence obtained was noted.

2.4. Data modeling

2.4.1. Combined severity factor

Regressions were created for all chemical, mass loss and spectral data as a function of the severity of the pretreatment, expressed as a combined severity factor (CSF, Eq. 2), commonly used for thermo-chemical pretreatment in industry (Auxenfans et al., 2017). Consequently, data from non-acidic samples were not used in this study, as CSF calculations are not interpretable for pH 7.

$$CSF = \log_{10}\left(t \times e^{\frac{T-Tr}{14.75}}\right) - pH \quad (2)$$

where t is the reaction time (min), T the operating temperature (°C), Tr the reference temperature (100°C) and pH is that of the acid liquid phase used to soak biomass.

2.4.2. Regressions

The graphical representations were obtained with SigmaPlot 14.5, which also allowed to plot the regressions of the data. The choice of the appropriate regression equation was made according to the shape of the data, with the objective of maximizing the value of the r^2 coefficients while keeping the equations as simple as possible. For each regression the full dataset was used, and no outliers were formally identified. For the regressions concerning mass loss and colorimetry, the use of linear equations made it possible to plot the confidence and prediction intervals. All the regressions, equations and coefficients associated are available online (see supplementary materials).

3. Results and discussion

3.1. Raw materials

Based on the analysis of the five raw samples, the average composition of dry untreated poplar was 46% cellulose, 22% hemicelluloses (including 17% xylose) and 20% lignin, which explains almost 90% of the total weight.

3.2. Sample mass losses

Mass loss follows a linear evolution with severity ($r^2 = 0.99$): from 0 for the lowest severity to 66.20% for the highest severity (Fig. 1D). This supports the good consistency of the pretreatments and the distribution of the data according to their severity, even if this indicator is not perfect (Ziegler-Devin et al., 2021). The evolution of the colorimetry also follows a linear variation (Fig. 1E), which might indicate that this parameter, easy to measure, could be a good synthetic indicator of the treatment intensity. As already suggested for estimating the energy quality of pellets (Lam et al., 2012; Pegoretti et al., 2019), the literature

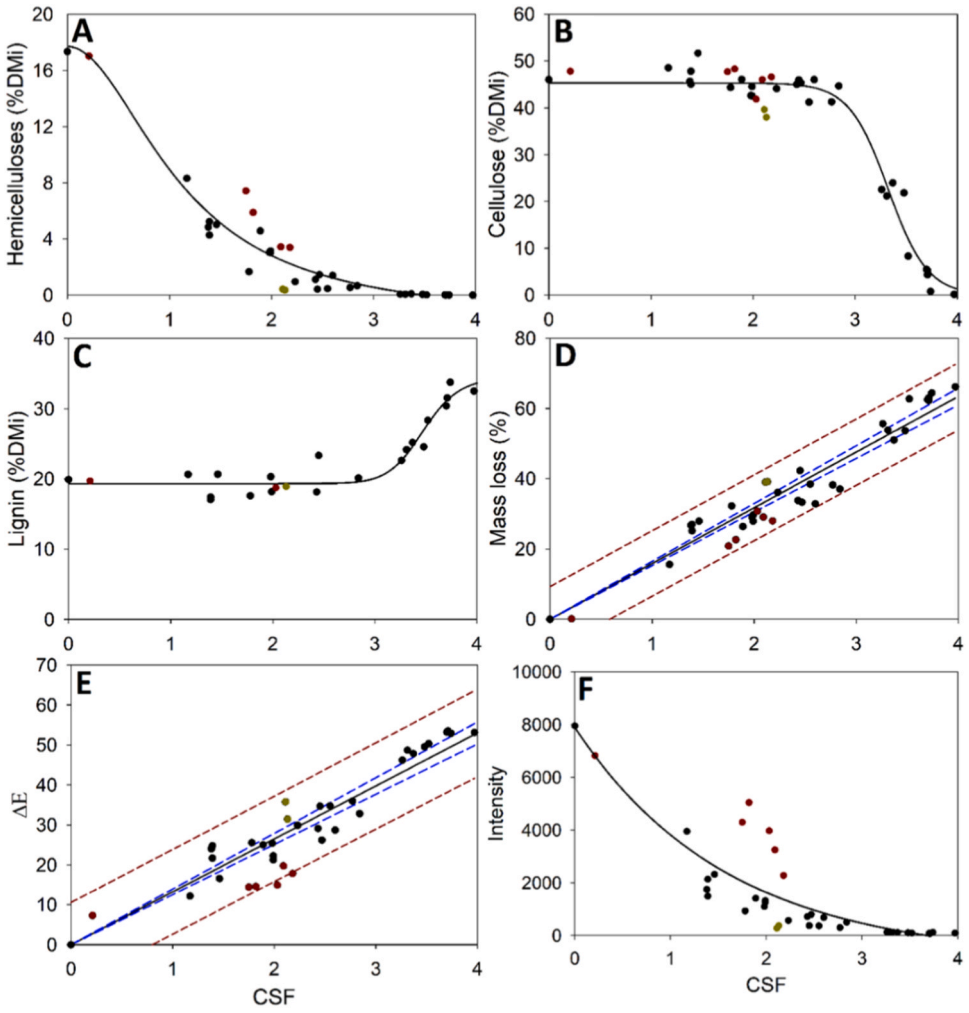

Fig. 1. Evolution of poplar wood composition subjected to DAP of increasing severity. A: Xylose in Hemicelluloses; B: Cellulose; C: Lignin; D: Mass loss; E: Color distance from raw poplar wood; F: Maximum intensity of emitted autofluorescence. Black dot: Data at conditions greater than 120°C and 2 min; Red dot: Data at 120°C conditions; Yellow dot: Data at 2 min conditions; Black line: Regression on all data; Blue dotted line: Confidence interval; Red dotted line: Prediction interval. (2-column fitting image, the color must be used for printing).

also supports good correlations between ΔE and lignin and xylan content of giant reed subjected to DAP, so that colorimetry could be used as a rapid measure of saccharification efficiency (Chen et al., 2023).

3.3. Chemical kinetics

3.3.1. Degradation of main wood compounds

A degradation of the main wood compounds is observed from low severities for hemicelluloses but requires a CSF value above 3 to obtain a significant degradation of cellulose, which is more resilient to pretreatment thanks to its crystalline and fibrils structures (Chundawat et al., 2011; Pu et al., 2013) (Fig. 1A, 1B). Like cellulose, the third main component of biomass, lignin, does not undergo any quantitative degradation before a CSF of 3 (Fig. 1C). Beyond this value, the amount of lignin increases to 150% yield, which denotes an artifact: the formation of pseudo-lignin. Actually, lignin can polymerize with the degradation products from HMF and furfural, and the whole is recognized as lignin by the Klason analysis (Rasmussen et al., 2014; Wan et al., 2019). Even if the quantity of lignin does not evolve until CSF 3, the intensity of autofluorescence (Fig. 1F), mainly influenced by aromatic groups present in lignin, decreases sharply with increasing CSF. This means that while the amount of lignin remains stable, its structure is easily and strongly modified at a low severity due to its redistribution in a more condensed form, even at 110°C (Assor et al., 2009; Pu et al., 2013).

3.3.2. Evolution of degradation products

Hemicelluloses and cellulose break down into xylose and glucose, respectively, and are released in the liquid phase (Fig. 2A, 2B). A maximum content is reached at CSF 2.2 and 3.4, before a complete degradation of sugars in furfural and HMF, respectively (Fig. 2C, 2D). These two compounds also display a maximum content, respectively at CSF 3.1 and 3.5. But the evolution of HMF shows very low levels, with a maximum of less than 1% DMi, while furfural reaches almost 5% DMi, for comparable xylose and glucose levels. These degradation pathways, as well as those of furfural, produce many different compounds, some of which have been identified and quantified: formic and succinic acid for furfural, levulinic and formic acid for HMF (Almhofer et al., 2023; Dulie et al., 2021; Dussan et al., 2013; Palmqvist and Hahn-Hägerdal, 2000; Rasmussen et al., 2014) (see supplementary materials).

3.4. Data accuracy

The study of the data according to their CSF made it possible to observe limits of precision for some data points corresponding to pretreatment conditions of 2 min and 120°C (Figs. 1 and 2 and supplementary materials, respectively yellow and red dot).

3.4.1. Pretreatment times too short

Indeed, the data at 2 min, corresponding to a CSF of 2.1, is positioned

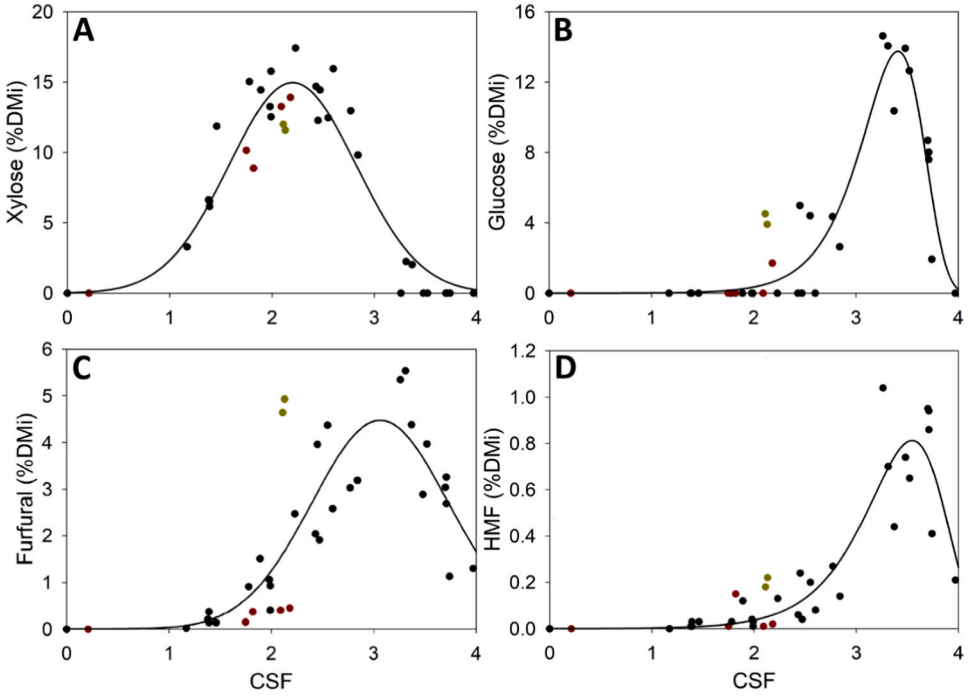

Fig. 2. Evolution of poplar wood degradation products dissolved in liquid phases subjected to DAP of increasing severity. A: Xylose solubilized; B: Glucose solubilized; C: Furfural; D: HMF. Black dot: Data at conditions greater than 120°C and 2 min; Red dot: Data at 120°C conditions; Yellow dot: Data at 2 min conditions; Black line: Regression on all data. *(2-column fitting image, the color must be used for printing)*.

recurrently far from the regressions (Figs. 1B, 2B, 2C). Given their position, it seems that the severity of these points is underestimated since it would be on the regression plot if the CSF value was shifted from 2.1 to around CSF 2.8, whatever the considered parameter. Indeed, in this reactor, the heating time to reach the target temperature is about 15 min, which can certainly not be neglected, especially for very short pretreatment durations. This effect is not considered in the calculation of the CSF, but it can be estimated on these points: maintaining the same acid and temperature conditions, changing the CSF from 2.1 to 2.8 requires an increase of the residence time from 2 to 9 min. Considering the start-up and temperature stabilization phases of the reactor, this corresponds to the heating time of 15 min.

3.4.2. *Pretreatment temperatures too low*

The data obtained at 120°C present an opposite problem, meaning the severity is slightly overestimated (Figs. 1A, 2C). This can be observed mainly on the colorimetry and autofluorescence intensity plots, with points very far from the data clouds (Figs. 1E, 1F). Given that these two measurements are strongly impacted by the properties of the lignin (they confer color and fluorescence to the sample), it would mean that 120°C is close to a threshold temperature (probably situated between 120°C and 140°C) where some important modifications of lignin can occur, regardless of the other conditions involved in the pretreatment. Keeping in mind that lignin modifications occur as early as 110°C (Assor et al., 2009), this threshold temperature is quite conceivable, and may even be overestimated. Despite these observations, all the points were kept for the calculation of the regressions.

3.5. *Degradation pathways*

To analyze these kinetics in greater detail, they were grouped into two main degradation pathways based on the number of carbon atoms of the chemical products involved. The first one is the C5 hemicellulosic degradation pathway, in which hemicelluloses are first depolymerized into xylose, then degraded into furfural, and two molecules resulting from its further degradation are measured, formic and succinic acids

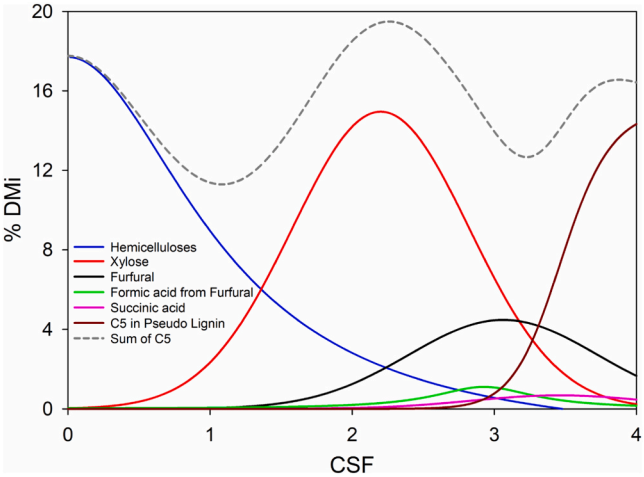

Fig. 3. Kinetics of formation and degradation of C5 compounds from poplar wood subjected to DAP with increasing severity. (2-column fitting image, the color must be used for printing).

(Fig. 3) (Dulie et al., 2021; Palmqvist and Hahn-Hägerdal, 2000; Rasmussen et al., 2014). The second pathway is the C6 cellulosic degradation pathway, in which cellulose is depolymerized into glucose, then degraded into HMF which itself produces equimolarly formic and levulinic acid (Fig. 4) (Dussan et al., 2013; Kim et al., 2021). Since lignin does not consist of sugars, it is not directly involved in these degradation pathways. However, the formation of pseudo-lignin implies the reaction of lignin with sugars and justifies the integration of lignin into the C5 and C6 pathways resulting from the degradation of HMF and furfural. As it is not possible to differentiate the C5 or C6 origin of the compounds included in the pseudo-lignin, and in order to simplify the visualization of these degradation pathways, the hypothesis was made that they come exclusively from the degradation of C5. This assumption is supported by two facts: i) the quantities of pseudo-lignin created are very close to the

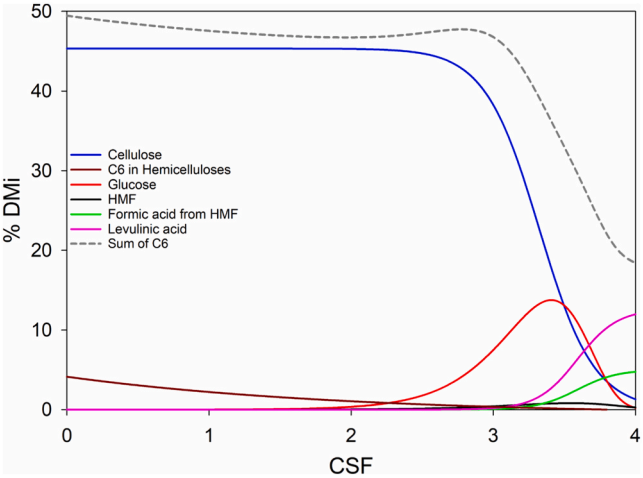

Fig. 4. Kinetics of synthesis and degradation of C6 compounds from poplar wood subjected to DAP with increasing severity. *(2-column fitting image, the color must be used for printing)*.

C5 losses observed (Fig. 3), and ii) C5 are only slightly involved in the formation of humin, the other most abundant degradation product (Rasmussen et al., 2014; Wan et al., 2019). Knowing the initial lignin content (20% DMi), the content of C5 included in the pseudo-lignin is obtained by subtraction. In the same way, to determine the C5 or C6 source of formic acid, the level of levulinic acid was considered: its formation from HMF leads to an equimolar formation of formic acid, and the remaining formic acid level is attributed to furfural (Dussan et al., 2013).

3.5.1. C5 degradation pathway

The C5 degradation pathway is quite complete, with a high confidence level regarding the evolution of compounds. The degradation of hemicelluloses begins for the early severities and is almost perfectly offset by the appearance of xylose in the liquid fraction (Fig. 3). The slight delay, observable by the dip of the sum of C5 at around CSF 1.1, is certainly due to the progressive conversion of hemicelluloses into xylo-oligosaccharides before becoming xylose monomers. A certain time delay is also required for these soluble sugars to be transferred into the liquid fraction. These oligosaccharides were not assayed in this study but could be estimated to represent up to 6% DMi, based on the decrease in the sum of C5 at CSF 1.1 compared with the initial amount of C5. The formation of xylose oligo-oligosaccharides is also described in the literature for DAP, where comparable maximum xylo-oligosaccharide levels of around 4.5% DMi are obtained for CSFs between 1 and 2 (Cuevas et al., 2015). Therefore, a CSF below 1.5 does not seem to be sufficient to completely degrade hemicelluloses into xylose. Maximum xylose content is reached close to CSF 2.2, which corresponds to the ranges observed in the literature: CSF 2.0–2.3 (Cuevas et al., 2015) or CSF 2.4–2.6 (Swiatek et al., 2020). For comparable biomass and pretreatment methods, the maximum rate of xylose obtained is also close to the initial rate in the raw biomass (Cuevas et al., 2015). Beyond these CSFs, xylose starts to degrade into furfural as well as into negligible amounts of succinic and formic acids. Finally, the massive loss of C5 in the formation of pseudo-lignin completes this degradation pathway above CSF 3.5 (Fig. 3).

A second significant drop in the sum of C5 is observed at CSF 3.2, which can be attributed to the large variety of compounds that can be produced from the degradation of biomass, in addition to levulinic, succinic and formic acids. For instance, corn stover subjected to DAP at CSF 3.1 shows more than 100 degradation compounds from different families: sugars, aromatics, carboxylic acids, furans, alcohols and aldehydes (Jiang et al., 2016). The C5 degradation products include many acids at trace levels (phthalic, lactic, caproic and furoic), the sum of which represents around 8% DMi (Jiang et al., 2016). This roughly corresponds to the missing 5% DMi observed in this study, based on the decrease in the sum of C5 at CSF 3.2 compared with the initial amount of C5 (Fig. 3).

3.5.2. C6 degradation pathway

The description of the C6 degradation pathway is easier for low and medium CSFs because the cellulose does not degrade yet (Fig. 4). Only C6 hemicelluloses were solubilized in the early stages of severity (CSF 0–2), but their content in the liquid fraction was not measured, resulting in a slight decrease in the sum of C6. After CSF 2.5, cellulose degrades very quickly. However, the amount of glucose measured in the liquid phase begins to increase earlier, at CSF 2. Even at its maximum, its content remains much lower than the initial amount of cellulose (Fig. 4). These observations are also validated by the literature, which shows glucose increase at CSF 2.25 and major cellulose degradation at CSF 2.54 (Cuevas et al., 2015), or a maximum glucose level attained for CSFs between 3.54 and 3.72 (Swiatek et al., 2020). The structure of cellulose, which includes a resistant crystalline structure (around 65%) and an amorphous phase more sensitive to DAP, may explain this phenomenon (Foston et al., 2009). The most exposed amorphous starts to degrade earlier around CSF 2, causing only a small variation in cellulose content (0–5% DMi, based on the amount of glucose produced between CSF 2 and 2.5). The remaining amorphous fraction and the crystalline parts require more drastic conditions at CSFs above 2.5, causing a drop in cellulose content as they degrade into glucose. These high CSFs are similar to those required for the degradation of glucose to HMF, which are also around CSF 2.5 (He et al., 2021). Glucose degradation therefore occurs very rapidly when the CSF is above 2.5, thus preventing its accumulation. However, despite the significant sources of cellulosic and hemicellulosic C6 (Palmqvist and Hahn-Hägerdal, 2000; Rasmussen et al., 2014), no HMF accumulation was observed at CSF above 2.5: it is only present as trace amounts below 1% DMi (Fig. 4). Higher yields of HMF have been obtained in the literature at comparable CSFs (Cuevas et al., 2015; Swiatek et al., 2020), but the acid levels in these works (0.25–0.5%wt) were much lower than those used in the present study for CSF $>$ 2.8 (1.5–6.8%wt). Since HMF is unstable in water under acidic conditions (Xue et al., 2016), it is immediately degraded into levulinic and formic acids, limiting its accumulation (Kim et al., 2021) in high CSF conditions.

Yet, it is important to note that levulinic and formic acid levels remain very low compared with the initial amount of cellulose (Fig. 4). It is likely that cellulose and glucose degrade directly into one or more non-analyzed compounds representing up to 30% DMi. These unknown products could be created for severe pretreatments where the formation of a blackish compound clogging the reactor is observed. First considered as being lignin, literature describes this compound as humin, a molecule resulting from the polymerization of glucose and HMF (Rasmussen et al., 2014). The small amount of glucose measured in high CSF conditions above 3 might therefore be explained by its direct degradation into humin. This also impacts the amount of HMF, because the reaction involved for its formation competes with that of humin.

3.6. Cascade of reactions pathway

Summarizing all the data, kinetics and hypotheses described in Figs. 3 and 4, a global mass balance scheme has been devised. In this scheme, the cascade of reactions pathway of the different compounds is related to the threshold CSF values at which the reactions occur (Fig. 5). The contents of each compound, indicated by the colored values, are taken from the maximum values obtained experimentally (Fig. 1 and 2). For humins and xylo-oligosaccharides, the values are estimations (purple compounds). For “other” compounds, contents are rated by the difference between the initial C5 or C6 values and the sum of the compounds at the corresponding CSF. For “Other C6”, the rate is based on the C6 content of the hemicelluloses. The cascade reactions start with

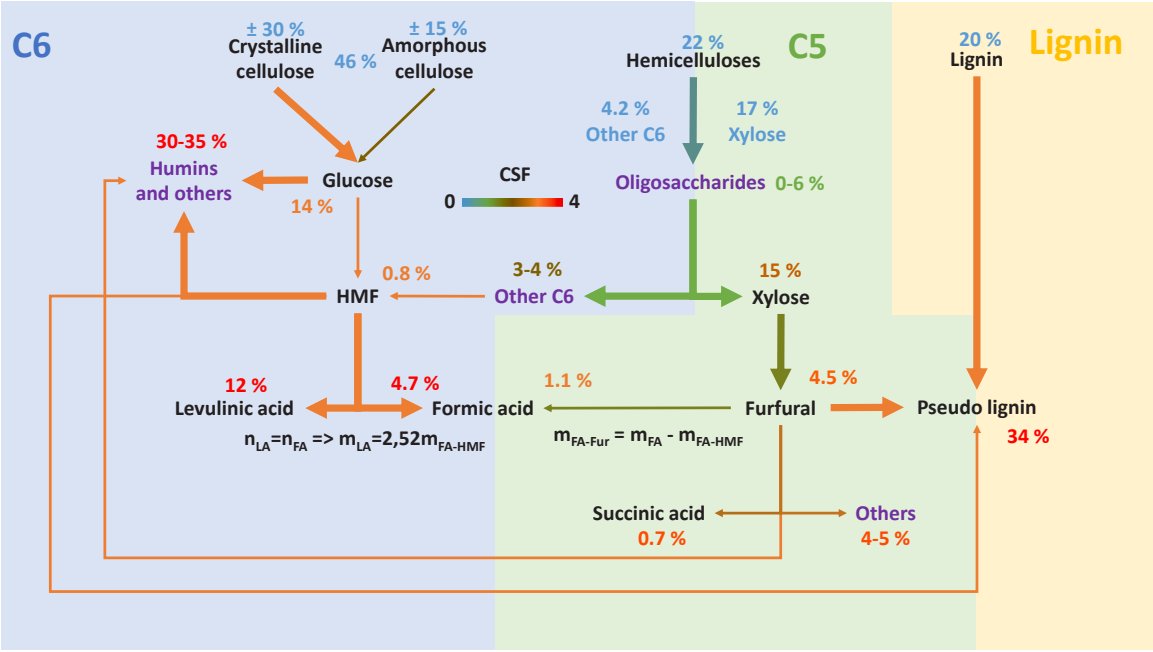

Fig. 5. Reaction diagram and mass balance of the degradation of poplar wood subjected to DAP. Thick arrows: Major pathway; Thin arrows: Minor pathway; Arrow color scale: Minimum CSF required for the reaction to occur; Blue percentage: Composition of initial dry mass; Other colored percentages: Maximum rate obtained in the liquid phase (%DMi) and corresponding optimal CSF; Purple compounds: Non-measured compounds. *(2-column fitting image, the color must be used for printing)*.

three main compounds of lignocellulosic biomass, along with their contents in poplar wood. Cellulose pathway is separated into two parts because the amorphous fraction (35% of total cellulose) begins its degradation at lower CSFs than the crystalline fraction (Foston et al., 2009). Hemicelluloses are the first to undergo degradation, starting at CSF 0 and extending up to 2.5, solubilizing into oligosaccharides and then into simple monomers (xylose or a mixture of C6) from CSF 1. Xylose degrades directly from CSF 1.5 into furfural, which in turn degrades to several molecules (formic acid, succinic acid and hundreds of other trace molecules (Jiang et al., 2016) from CSF 2. But the most important changes begin at CSF 3: all C5 monosaccharides likely start to bind with lignin to form pseudo-lignin while cellulose solubilizes very rapidly into glucose. A fraction of the glucose and hemicellulosic C6 are degraded into levulinic and formic acids through HMF, while the rest of the sugars complex with HMF to form humins or other unidentified molecules, corresponding to the sum of hundreds of trace molecules not analyzed in this study (Jiang et al., 2016). It is possible that the humin contains a part of furfural, and pseudo-lignin is also made up of a fraction of HMF (or products of their degradation). These two macromolecules are not very well characterized, and can't even be completely dissociated (Rasmussen et al., 2014; Wan et al., 2019). What is important is that at very high CSFs, these two prevalent molecules represent more than 65% of the initial dry mass. Beyond their inhibitory effect (Rasmussen et al., 2014), they are responsible for significant yield losses: up to 50% of C5 and 40% of C6 are lost at the severe conditions tested. The use of CSF greater than 3 is therefore not recommended in the case pretreatment of the biomass is considered prior to enzymatic hydrolysis and/or fermentation. In view of the large number of chemical reactions involved in these degradation pathways, it is obvious that the mass balance cannot be complete. Indeed, water and some volatiles, including CO_2, are also produced but were not assayed. However, these degradations only happen at very high severity values, and preferentially in the presence of catalyst (Kim et al., 2021), so the quantities involved are certainly negligible.

This study provides the most comprehensive overview to date of the degradation process of poplar wood compounds exposed to DAP. It provides a research base for future academic or industrial scale-up projects to optimize their pretreatment according to their production goals by using these data as a guide for selecting the appropriate severity of DAP. For example, the use of CSF greater than 3 does not seem to be of any interest in the context of pretreatment of the biomass prior to enzymatic hydrolysis and/or fermentation since it leads to massive losses of C5 and C6. On the other side, pretreatment at CSF below 1 has no interest, as even hemicelluloses are not completely degraded, and remain as oligosaccharides. This leaves a CSF work range from 1 to 3, with very interesting CSFs for enzymatic hydrolysis steps between 2 and 2.5: hemicelluloses are completely degraded, as well as an amorphous fraction of the cellulose, but without formation of inhibitors, except a small content of furfural. This leaves the crystalline part of the cellulose available for hydrolysis and should therefore enable high glucose yields to be obtained. By using CSFs just below 3, it is also possible to maximize furfural production because its degradation has not yet begun. Its role as an intermediate platform molecule for several reactions makes it very interesting from an industrial point of view.

4. Conclusion

This study proposes the most comprehensive overview of the cascade reactions and chemical interactions that occur within poplar wood during pretreatment. This quantified severity-based yield analysis was derived from the analysis of a broad dataset, covering an unprecedented range of conditions and including numerous chemical and spectral analyses. All these data were combined into a complete reaction scheme that can be used as a decision-making tool to tune the treatment conditions depending on the expected objective. For example, the production of glucose after enzymatic hydrolysis, a major goal for the valorization of LB, requires CSFs around 2–2.5 to allow almost complete degradation of hemicelluloses into xylose without altering the cellulose or producing inhibitors. The use of a CSF slightly lower than 3 can also be interesting for furfural production. However, the use of a CSF greater than 3 is not recommended as it results in a loss of 50% and 40% of C5 and C6 in pseudo-lignin and humins, respectively. As further works, enzymatic hydrolysis analyses could be interesting to confirm these results.

Funding source

J. du Pasquier's PhD was funded by Grand Reims and Chaire de Biotechnologie de CentraleSupélec.

CRediT authorship contribution statement

Patrick Perré: Writing – review & editing, Visualization, Project administration, Funding acquisition, Conceptualization. **Gabriel Paës:** Writing – review & editing, Visualization, Project administration, Funding acquisition, Conceptualization. **Julien du Pasquier:** Writing – original draft, Visualization, Validation, Methodology, Investigation, Formal analysis, Data curation, Conceptualization.

Declaration of Competing Interest

The authors declare that they have no known competing financial interests or personal relationships that could have appeared to influence the work reported in this paper.

Data Availability

Data are fully accessible in a repository.

Acknowledgments

The authors would like to thank the Département de la Marne, Grand Reims, Région Grand Est and the European Union along with the European Regional Development Fund (ERDF Champagne Ardenne 2014–2020) for their financial support of the Chair of Biotechnology of CentraleSupélec.

Supplementary material

E-supplementary data for this work can be found in e-version of this paper online.

Appendix A. Supporting information

Supplementary data associated with this article can be found in the online version at doi:10.1016/j.indcrop.2024.118643.

References

Acosta, A.M., Cosovanu, D., Lopez, P.C., Thomsen, S.T., Gernaey, K.V., Canela-Garayoa, R., 2021. Co-cultivation of a novel Fusarium striatum strain and a xylose consuming Saccharomyces cerevisiae yields an efficient process for simultaneous detoxification and fermentation of lignocellulosic hydrolysates. Chem. Eng. J. 426, 131575 https://doi.org/10.1016/j.cej.2021.131575.

Almhofer, L., Bischof, R.H., Madera, M., Paulik, C., 2023. Kinetic and mechanistic aspects of furfural degradation in biorefineries. Can. J. Chem. Eng. 101, 2033–2049. https://doi.org/10.1002/cjce.24593.

Assor, C., Placet, V., Chabbert, B., Habrant, A., Lapierre, C., Pollet, B., Perre, P., 2009. Concomitant changes in viscoelastic properties and amorphous polymers during the hydrothermal treatment of hardwood and softwood. J. Agric. Food Chem. 57, 6830–6837. https://doi.org/10.1021/jf901373s.

Auxenfans, T., Cronier, D., Chabbert, B., Paës, G., 2017. Understanding the structural and chemical changes of plant biomass following steam explosion pretreatment. Biotechnol. Biofuels 10, 36. https://doi.org/10.1186/s13068-017-0718-z.

Becker, J., Wittmann, C., 2019. A field of dreams: lignin valorization into chemicals, materials, fuels, and health-care products. Biotechnol. Adv. 37, 107360 https://doi.org/10.1016/j.biotechadv.2019.02.016.

Beig, B., Riaz, M., Naqvi, S.R., Hassan, M., Zheng, Z.F., Karimi, K., Pugazhendhi, A., Atabani, A.E., Chi, N.T.L., 2021. Current challenges and innovative developments in pretreatment of lignocellulosic residues for biofuel production: a review. Fuel 287, 119670. https://doi.org/10.1016/j.fuel.2020.119670.

Chen, B.W., Kan, Y.N., Zhai, S.C., Mei, C.T., Huang, C.X., Yong, Q., 2023. Unveiling the mechanism of various pretreatments on improving enzymatic hydrolysis efficiency of the giant reed by chromatic analysis. Biomass-.-. Convers. Biorefinery 13, 2151–2161. https://doi.org/10.1007/s13399-021-01299-y.

Chen, J.X., Zhang, B.Y., Luo, L, L., Zhang, F., Yi, Y.L., Shan, Y.Y., Liu, B.F., Zhou, Y., Wang, X., Lu, X., 2021. A review on recycling techniques for bioethanol production from lignocellulosic biomass. Renew. Sust. Energ. Rev. 149, 111370 https://doi.org/10.1016/j.rser.2021.111370.

Chundawat, S.P.S., Beckham, G.T., Himmel, M.E., Dale, B.E., 2011. Deconstruction of Lignocellulosic Biomass to Fuels and Chemicals. In: Prausnitz, J.M. (Ed.), Annual Review of Chemical and Biomolecular Engineering. Annual Reviews. Palo Alto, pp. 121–145.

Cuevas, M., Sánchez, S., García, J.F., Baeza, J., Parra, C., Freer, J., 2015. Enhanced ethanol production by simultaneous saccharification and fermentation of pretreated olive stones. Renew. Energy 74, 839–847. https://doi.org/10.1016/j.renene.2014.09.004.

Dulie, N.W., Woldeyes, B., Demsash, H.D., Jabasingh, A.S., 2021. An insight into the valorization of hemicellulose fraction of biomass into furfural: catalytic conversion and product separation. Waste Biomass Valoriz. 12, 531–552. https://doi.org/10.1007/s12649-020-00946-1.

Dussan, K., Girisuta, B., Haverty, D., Leahy, J.J., Hayes, M.H.B., 2013. Kinetics of levulinic acid and furfural production from Miscanthus x giganteus. Bioresour. Technol. 149, 216–224. https://doi.org/10.1016/j.biortech.2013.09.006.

Foston, M., Hubbell, C.A., Davis, M., Ragauskas, A.J., 2009. Variations in cellulosic ultrastructure of poplar. BioEnergy Res 2, 193–197. https://doi.org/10.1007/s12155-009-9050-1.

He, O.W., Zhang, Y.F., Wang, P., Liu, L.N., Wang, Q., Yang, N., Li, W.J., Champagne, P., Yu, H.B., 2021. Experimental and kinetic study on the production of furfural and HMF from glucose. Catalysts 11, 11. https://doi.org/10.3390/catal11010011.

Jiang, F.X., Zhou, X., Xu, Y., Zhu, J.J., Yu, S.Y., 2016. Degradation profiles of non-lignin constituents of corn stover from dilute sulfuric acid pretreatment. J. Wood Chem. Technol. 36, 192–204. https://doi.org/10.1080/02773813.2015.1112403.

Kim, J.-H., Choi, J.-H., Kim, J.-C., Jang, S.-K., Kwak, H.W., Koo, B., Choi, I.-G., 2021. Production of succinic acid from liquid hot water hydrolysate derived from Quercus mongolica. Biomass Bioenergy 150, 106103. https://doi.org/10.1016/j.biombioe.2021.106103.

Lam, P.S., Sokhansanj, S., Bi, X.T., Lim, C.J., 2012. Colorimetry applied to steam-treated biomass and pellets made from western douglas fir (Pseudotsuga menziesii l.). Trans. Asabe. 55, 673–678. https://doi.org/10.13031/2013.41368.

Palmqvist, E., Hahn-Hägerdal, B., 2000. Fermentation of lignocellulosic hydrolysates. II: inhibitors and mechanisms of inhibition. Bioresour. Technol. 74, 25–33. https://doi.org/10.1016/S0960-8524(99)00161-3.

du Pasquier, J., 2022. Chemical composition of solid and liquid phases resulting from dilute acid pretreatment of poplar wood under different conditions. Data.gouv, v1. ⟨https://www.data.gouv.fr/fr/datasets/chemical-composition-of-solid-and-liquid-phases-resulting-from-dilute-acid-pretreatment-of-poplar-wood-under-different-conditions/⟩..

du Pasquier, J., Paës, G., Perré, P., 2023a. Principal factors affecting the yield of dilute acid pretreatment of lignocellulosic biomass: a critical review. Bioresour. Technol. 369, 128439 https://doi.org/10.1016/j.biortech.2022.128439.

du Pasquier, J., Perré, P., Paës, G., 2023b. Construction and exploration of a dilute acid pretreatment dataset on poplar wood to propose trade-offs of chemicals evolution. Bioresour. Technol. Rep. 24, 101636 https://doi.org/10.1016/j.biteb.2023.101636.

Pegoretti, H.J., Chaves, M.D., Vidaurre, G.B., Brocco, V.F., de Souza, D.P., Protasio, T.D., 2019. Colorimetry of pellets produced with eucalyptus and coffee cultivation residues and their relationship to quality standards. Sci 47, 114–124. https://doi.org/10.18671/scifor.v47n121.11.

Pu, Y.Q., Hu, F., Huang, F., Davison, B.H., Ragauskas, A.J., 2013. Assessing the molecular structure basis for biomass recalcitrance during dilute acid and hydrothermal pretreatments. Biotechnol. Biofuels 6, 15. https://doi.org/10.1186/1754-6834-6-15.

Rasmussen, H., Sorensen, H.R., Meyer, A.S., 2014. Formation of degradation compounds from lignocellulosic biomass in the biorefinery: sugar reaction mechanisms. Carbohydr 385, 45–57. https://doi.org/10.1016/j.carres.2013.08.029.

RFA, Renewable Fuels Association, 2023. Annual Ethanol Production: U.S. and World Ethanol Production. ⟨https://ethanolrfa.org/markets-and-statistics/annual-ethanol-production⟩ (accessed 23/03/2023).

Ritchie, H., Roser, M., Rosado, P., 2022. Energy, Our World in Data. ⟨https://ourworldindata.org/energy⟩ (accessed 24/08/2023).

Swiatek, K., Gaag, S., Klier, A., Kruse, A., Sauer, J., Steinbach, D., 2020. Acid hydrolysis of lignocellulosic biomass: sugars and furfurals formation. Catalysts 10, 437. https://doi.org/10.3390/catal10040437.

Tan, J.Y., Li, Y., Tan, X., Wu, H.G., Li, H., Yang, S., 2021. Advances in pretreatment of straw biomass for sugar production. Front Chem. 9, 696030 https://doi.org/10.3389/fchem.2021.696030.

Wan, G.C., Zhang, Q.T., Li, M.F., Jia, Z., Guo, C.Y., Luo, B., Wang, S.F., Min, D.Y., 2019. How pseudo-lignin is generated during dilute sulfuric acid pretreatment. J. Agric. Food Chem. 67, 10116–10125. https://doi.org/10.1021/acs.jafc.9b02851.

Xue, Z.M., Ma, M.G., Li, Z.H., Mu, T.C., 2016. Advances in the conversion of glucose and cellulose to 5-hydroxymethylfurfural over heterogeneous catalysts. RSC Adv. 6, 98874–98892. https://doi.org/10.1039/c6ra20547j.

Yoo, C.G., Meng, X., Pu, Y., Ragauskas, A.J., 2020. The critical role of lignin in lignocellulosic biomass conversion and recent pretreatment strategies: a comprehensive review. Bioresour. Technol. 301, 122784 https://doi.org/10.1016/j.biortech.2020.122784.

Ziegler-Devin, I., Chrusciel, L., Brosse, N., 2021. Steam explosion pretreatment of lignocellulosic biomass: a mini-review of theorical and experimental approaches. Front Chem. 9 https://doi.org/10.3389/fchem.2021.705358.